

# Nanoparticles by chemical synthesis, processing to materials and innovative applications<sup>†</sup>

Helmut Schmidt\*

Institut für Neue Materialien, Im Stadtwald, Gebaeude 43, 66123 Saarbruecken, Germany

---

Nanoparticles have been fabricated by using chemical synthesis routes under specific conditions. During a precipitation process from liquid phases, surface controlling agents (SCAs) have been added during or shortly after the formation of precipitates. These interfere with the nucleating and growing particle to avoid agglomeration and to control size. Nanoparticles from many systems have been fabricated. If the SCAs are bifunctional, the surfaces chemistry could be tailored and the zeta potential of these particles was tailored also. SiO<sub>2</sub> particles have been used for gene targeting using this approach. In other investigations, FeO<sub>x</sub> nanoparticles have been surface modified by amino groupings together with a sonochemical route to obtain very stable coatings. These particles have been used for *in vitro* tumor cell penetration and hyperthermal treatment. Boehmite nanoparticles were used to serve as condensation catalysts to prepare very hard transparent coatings for polycarbonate and an overcoat with polymerizable nanoparticles was used to produce anti-reflective and ultrahard coatings. In systems with incorporated fluoro silanes, leading to low surface free energy coatings, nanoparticles were used to tailor the fluorine depth profile in self-aligning transparent easy-to-clean coatings by influencing the critical micelle concentration. The examples show the usefulness of the chemical nanoparticle approach for nanocomposite fabrication and the high potential of these materials for medical and industrial application. Copyright © 2001 John Wiley & Sons, Ltd.

**Keywords:** nanoparticles; colloids; nanocomposites; wet coating

## 1 INTRODUCTION

Nanostructured materials have been of interest since the early 1980s and are mainly based on papers where metallic nanoparticles have been prepared by various gas-phase or vacuum methods, and then are densified to nanostructured solids.<sup>1–5</sup> These materials showed very interesting properties that have been attributed to the high volume fraction of interfacial structures that are different from the crystalline structures of the core. The investigations have been extended to ceramics, where Niihara,<sup>6</sup> in particular, has carried out many investigations on ceramic nanocomposites, and very interesting properties with respect to toughness and strength have been reported. However, despite the high very interesting potential of ceramic nanostructured materials, with a few exceptions, no broad industrial breakthrough has taken place so far, despite the fact that many companies have tried to commercialize these concepts.

On the other hand, nanostructured powders obtained by a flame pyrolysis process have been commercial products for a long time, e.g. SiO<sub>2</sub> or TiO<sub>2</sub> (Aerosil<sup>®</sup>, Cab-o-sil<sup>®</sup>). Nanoparticles, through colloidal chemistry in liquid environments, play a role in many processes in nature, in industrial processes (e.g. the fabrication of water glass), and also in biology.<sup>7</sup> Typical colloids are representative of nanoparticles stabilized in solution in order to prevent aggregation. The stabilization, in general, takes place by the absorption of electric charges on the surface, leading to a repulsion of the nanoparticles as long as a critical distance is maintained. This phenomenon was investigated by Stern at the beginning of the 20th century.<sup>8</sup> The utilization of the colloidal route leads to interesting concepts for the preparation of new nanostructured materials. For this reason, many investigations have been carried out on the so-called colloidal processing of ceramics through sol–gel routes. Bowen and co-workers at MIT developed routes for colloidal

---

\* Correspondence to: H. Schmidt, Institut für Neue Materialien, Im Stadtwald, Gebaeude 43, 66123 Saarbruecken, Germany.  
E-mail: schmidt@inm-gmbh.de

<sup>†</sup> Based on work presented at the 1st Workshop of COST 523: Nanomaterials, held 20–22 October 1999, at Frascati, Italy.

processing of ceramics by centrifugation or pressure filtration,<sup>9</sup> but it was very difficult to obtain sufficient green density through these routes. The reason for this is that during the up-concentration of the colloids, according to Stern's model, after the particle distance becomes smaller than the critical distance, the repulsion changes into attraction; this leads to the formation of strong bonds between the colloidal particles and a random network formation that is characterized by a high porosity takes place. This leads to low green densities with a bimodal pore size distribution; the result is a two-step sintering process with the closure of the small pores and the enlargement of the large pores, and the benefit of the small particles vanishes through this effect.<sup>10</sup> For this reason, the high expectations attributed to colloidal routes for making ceramics could not be fulfilled and colloidal processing became rather unattractive in the past.

Nanoparticles and nanocomposites prepared by precipitation or *in situ* formation in a given matrix through the sol-gel processes have been investigated for more than 10 years.<sup>11–81</sup> This is an interesting route for the fabrication of nanocomposites by chemistry. In all these investigations, very similar principles using alkoxides as a basis are used. The idea of  $\zeta$ -potential tailoring or surface modification for compatibilization or specific reactivity is only discussed in a very few papers. Almost no data about processing and product development are given. In order to obtain a sufficient dispersion the particle surface has to be compatibilized to the matrix, and surface modification of the nanoparticles becomes an indispensable means for the development of appropriate processing routes, or, as in the case that reactive monomers are introduced into a given polymer, nucleation and growth have to be controlled. Another area of nanocomposites with polymer matrices is clay-based systems.<sup>82–84</sup>

In the present paper, various aspects of nanoparticles and nanoparticle fabrication are discussed. The main objective of this paper, however, is to show how basic results of sol-gel and colloidal chemistry can be used for industrial product development. The sol-gel process, praised as a route for the fabrication of novel materials with a tremendous application potential now for more than two decades, has not fulfilled the expectations by far. Only in Japan, where many product-developing industries have their own chemistry departments or can share developments of in-house chemical companies, is the situation quite different, and many products are on the market.<sup>85</sup> For this reason,

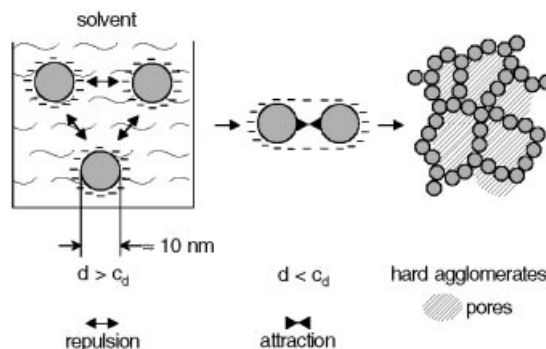


**Figure 1** Scheme of the formation of agglomerates from colloidal sols (sol-gel transition).

several examples for the preparation of materials are chosen, and it is shown, how by appropriate processing technologies industrial applications have been developed starting from very basic results. The preparation of nanocomposites by chemistry will be summarized and a short overview of some developments for materials for industrial applications will be given. In these systems, an intercalation process is required to delaminate the stacks, which seems to be possible for many polymers. The concentration seems to be limited to about 15 vol.% due to the platelike shape of the clay.

## 2. GENERAL CONSIDERATIONS FOR COLLOIDAL ROUTES TO NANOPARTICLES

The concept of fabricating nanoparticles by a simple precipitation process seems to be intriguing. But to overcome the problem of aggregation or growth to micrometer-sized particles, and to obtain processable particles, new concepts had to be developed. The inorganic colloidal route is a special case of a precipitation process with nucleation and growth to amorphous or crystalline

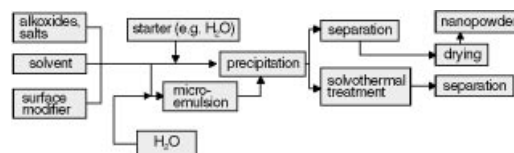


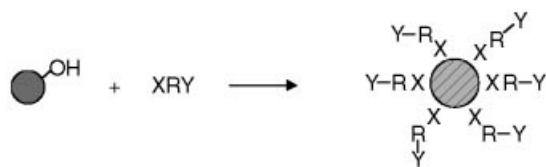
**Figure 2** General scheme of a chemical route to nanoparticles (after Refs 96 and 99).

particles. If the concentration of the feed is low and the pH value of the solution is in a range that surface charges are generated, colloidal particles with diameters in the lower nanometer range are accessible. This has been shown by Matijevich and Her for many systems in very diluted solutions.<sup>86–88</sup> The basics of these processes are also discussed in the book by Scherer and Brinker.<sup>89</sup> The utilization of the colloidal state-of-the-art for the production of nanostructured materials, however, was not a matter of detailed investigations in the field of sol–gel chemistry. However, recent investigations including microwave and hydrothermal processing have been used for nanoparticle systems.<sup>4</sup> One of the serious problems is the strong aggregation during processing from sols to gels. This is shown in Fig. 1, where the formation of low-density aggregates is demonstrated. The intriguing perspective, however, is that through simple precipitation processes a wide variety of composition is available, ranging from simple oxides to chalcogenides or even metals.<sup>90–95</sup>

For these reasons, a precipitation route under a growth-controlling condition has been developed.<sup>96–98</sup> This process is based on the hypothesis that molecules able to interact with the particle surface are influencing nucleation and growth through the interfacial free energy. It could be shown that the growth reaction follows rather simple rules.<sup>99</sup> It also could be shown that by use of surface-controlling agents, very uniform particle sizes in the nanometer range could be obtained. Various types of component can be used as growth and size-controlling agents, e.g. complex-forming agents as  $\beta$ -diketones, which are very useful for oxides, other complex ligands, like amines or chelating agents, which have shown their usefulness for metals,<sup>100</sup> or sulfides in the case of chalcogenides like  $\text{CdS}_2$ .<sup>101,102</sup> It is postulated that these components control the surface free energy during the nucleation and growth process in a way that very uniform particle size distributions are obtained. This can be explained by assuming that an optimal coverage of the surface with the surface modifier exists that is specific for a given system (leading to a free energy minimum), and that an exchange of ions or molecules between the particle can take place. In this case, as shown in Ref. 97., the particle size can be tailored by the feed-to-ligand (surface-controlling agent, SCA) ratio. In only a few papers, however, was an attempt made to fabricate materials based on nanoparticles.<sup>100,101</sup>

Based on these considerations, a generalizable process has been developed for the fabrication of

nanoparticles that is shown schematically in Fig. 2 and described in detail.<sup>96</sup> In this process, liquid precursors are used, which, as a rule, react with water in the presence of  $\text{H}^+$  or  $\text{OH}^-$  and a specific SCA to the corresponding precipitates. For multi-component systems, diphasic systems, e.g. micro-emulsions, are preferred.<sup>98</sup> After precipitation, separation processes like centrifugation or filtration follow, after changing the zeta-potential to obtain weak and reversible aggregation. After precipitation, a composition like  $\text{Y-ZrO}_2$  is only poorly crystallized. By employing the hydro- or solvothermal process described in detail in the experimental part in Ref. 103, fully crystallized nanoparticles of about 10 nm in diameter are obtained. Similar results have been obtained by Komarneni and coworkers.<sup>104,105</sup> The surface modifiers fulfill several requirements: they not only control nucleation and growth, they also prevent the agglomeration and they provide a desired surface chemistry for further processing. This is shown schematically in Fig. 3 (bifunctional molecule or SCA approach). As shown by Sanchez *et al.*<sup>106</sup> or Naß and Schmidt,<sup>107</sup>  $\beta$ -diketones are suitable for surface modification, but no data with respect to materials synthesis are given. The surface chemistry employed is basically not different from the well-known chemistry taking place on all types of solid surface with reactive molecules. However, there is a quantitative difference, since solid surfaces, in general (with the exception of highly porous adsorbents), only show the geometric surface, which is distinctively below  $1 \text{ m}^2 \text{ g}^{-1}$ . Nanoparticles in the range of 10 nm in diameter, however, show specific surface areas of several hundred square meters per gram. This means the contribution of the surface modifiers to the chemistry of the nanoparticles is several orders of magnitude larger than on common solid surfaces. This also means that the surface modifiers influence the chemical nature of the nanoparticles remarkably, but, if small molecules are used, they do not contribute very much to the volume or the weight of these particles. As is well known from Ref. 1, nanoparticles are characterized by a large volume fraction of ‘disordered’ shell; the additional surface modification leads to a three-phased system, consisting of a well-ordered core, a less ordered shell and an organic thin cover layer. As shown in section 3.1, the coatings made from these particles show very interesting properties with respect to densification. The ‘construction principle’ of this type of new material is shown in Fig. 4. The assumption is made that the organic layer is able to reduce the particle



XRY = bifunctional molecule, SCA

X = binding grouping ( $\beta$ -diketones, complex formers, reactive silanes, acids etc.)

R =  $\equiv$  Si -, hydrocarbon groupings

Y = reactive and non-reactive or functional groupings (complex formers, acids, bases, epoxides, double bonds, aryl or alkyl groupings)

**Figure 3** Scheme of surface modifying and tailoring of surface chemistry of nanoparticles (SCA concept).

to particle interaction and to allow a 'gliding' of one particle on the others surface. It is expected that a denser packing than with uncoated particles is obtained. Gels or layers prepared from unmodified sols, in general, are porous due to the brittleness of the structure. In addition to the surface chemistry, the surface modifiers also may be used to tailor the surface charge of the particles. In this case, the modifiers have to be ionic, e.g. by use of amino groupings. The surface charges are, for example, measured by acoustophoretic measurement, which is a very fast analytical method monitoring the surface charge. Since the surface charge, in general, is dependent on pH, the zeta potential (indicating the quantity of surface charges), as a rule, is measured as a function of the pH. The effect of amino grouping modification of  $\text{SiO}_2$  on the zeta

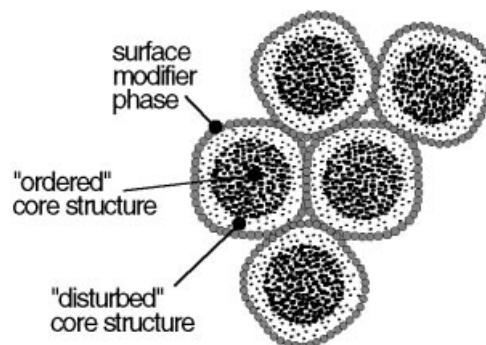


**Figure 4** Structural model of a Nanomer<sup>®</sup>-type of inorganic-organic nanocomposite.

potential is shown in Fig. 5. As one can see clearly, the zeta potential is shifted considerably to positive values, and, what is remarkable, at neutral pH a high positive value is still maintained. This principle has been used to fabricate  $\text{SiO}_2$  nanoparticles for the binding of nucleic acid plasmids for transfecting them into living cells.<sup>108,109</sup> The stabilization at pH 7 is of importance for the processing of sols, for example in industrial coating technologies where especially the use of acids to stabilize sols leads to corrosion problems of equipment. Using this approach, neutral sols have been prepared from  $\text{SiO}_2$  and  $\text{SiO}_2$ -Au sols<sup>110</sup> for dip coating purposes on glass. During firing at 450 to 500 °C, gold complexes made from  $\text{Au}^{3+}$  and  $\gamma$ -aminopropyltriethoxysilane form gold nanoparticles to produce the well-known gold ruby color. Nanoparticles show the potential of introducing specific properties into a given matrix. Table 1 shows a survey over basic properties and their potential for application. It becomes clear that, for

**Table 1** Some examples for properties and applications of nanostructured materials

Basic properties		Physical effect	Application
Small size	low light scattering		optical composites with transparent matrix
Small size	high specific surface area		low sintering ceramics, catalysts
	electron/hole formation		photocatalytic activity/ $\text{TiO}_2$ NLO in semiconductors
Quantum effects	plasmon resonance		NLO in metal colloids, colors
Small size	reinforcement high interface volume fraction		polymer matrix nanocomposites (hard, transparent, abrasion resistant, functional)
Size effect	ferromagnetic $\rightarrow$ superparamagnetic properties		magneto-fluids, energy and separation systems
Small size	high excess energy		low sintering ceramics, ceramic coatings, ceramic additives
Small size	transfectability into living cells		gene targeting, transport vehicles into cells

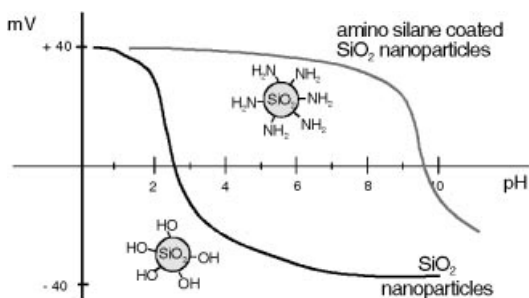


**Figure 5** Effect of amino groupings as surface modifier on the zeta-potential curve of colloidal  $\text{SiO}_2$  (after Ref. 108).

the utilization of this potential, many developments towards materials and processes are required.

By a combination of the solid-state properties of the nanoparticles with properties obtained by the surface modification and a polymeric glass-like or ceramic matrix, an interesting material-tailoring concept for nanostructured materials has been developed. As one can see from Table 1, there are many possibilities for the development of interesting applications based on nanoparticles. This, of course, is only a small section, but this indicates the wide range of possibilities.

### 3. EXAMPLES FOR PRODUCT DEVELOPMENTS

#### 3.1 Development and processing of magnetic nanoparticles

Iron oxides, such as magnetite or maghemite, are ferromagnetic if multidomain structures are present. By employing an external magnetic field, the domains become aligned and, by influencing each other, they also maintain a permanent magnetic field when the external magnetic field is switched off.  $\text{Fe}_2\text{O}_3$  particles of this type of microstructure show a strong hysteresis and are used for many applications, like magnetic recording. The coupled spins in the domains, however, have to fight against the Brownian movement, and in single domain systems, if the domain size gets below 10 to 6 nm, Brownian movement at room temperature destroys the spin coupling. This means that, after switching off the external magnetic field, the magnetism disappears and no hysteresis is to be found (superparamagnetism). Particle sizes distinctively above 10 nm show a multidomain structure with a

permanent magnetism. This leads to an attraction of the particles and to aggregation. These aggregates, however, are too large for some interesting applications, for example for the transport of such particles into living cells. For this reason, single-domain particles with surface properties to keep them stable at pH 7 have been developed.

Well-crystallized iron oxide particles can be easily obtained by precipitation.<sup>111–114</sup> However, in general, these particles are strongly agglomerated, and it is extremely difficult to obtain completely redispersed distributions in the primary particle size between 6 and 10 nm with a single-domain structure.  $\text{Fe}_2\text{O}_3$  shows a zeta potential with a point of zero charge close to neutral; this means that these particles flocculate or aggregate at neutral and cannot be used in a biological environment. In Ref. 115, a process is described where  $\text{FeO}_x$  particles have been precipitated in presence of aminosilanes. This leads to amino-grouping-coated  $\text{FeO}_x$  particles. Owing to the weak bonding of  $\equiv\text{SiOH}$  groupings to the surface of  $\equiv\text{FeOH}$ , the stability of the suspension is only maintained at low pH values. To use such suspensions under neutral conditions, a hydrolytically stable coating with a zeta potential at pH 7 high enough to avoid flocculation or agglomeration has to be established. To obtain an amino grouping modification more stable than described in Ref. 115, a sonochemical process, the details of which are described elsewhere, has been developed; this is shown in Fig. 6, according to Refs 116 and 117. In this process, a precipitation step has led to weak agglomerates. After precipitation, amino silanes and ethylene glycol have been added and the system is treated with ultrasound. As one can see from Fig. 7, during this treatment, the average particle size is reduced remarkably and, at the same time, the particles are coated by the amino silane. The self-condensation

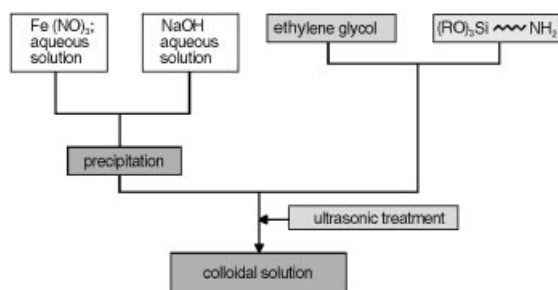


**Figure 6** Scheme of the precipitation and redispersion process under sonochemical conditions.

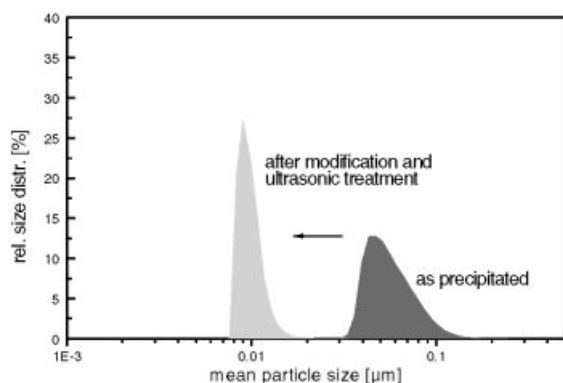


**Figure 7** Reduction of particle size by ultrasonic treatment.

of the amino silane is carried out under conditions where ultrasonic energy is used to enhance the condensation, which leads to a very stable coating. Without ultrasonic treatment, a simple reaction of the iron nanoparticles with the amino silane does not lead to a chemically stable coating. The ultrasonic treatment leads to a stability between pH 1 and pH 11 over a long period without change of the zeta potential curve (testing period 12 h). Through the amino silane treatment, the zeta potential of the system is shifted to higher pH values, so that at pH 7 a zeta potential of about 40 mV exists, as shown in Fig. 8; it results in very stable colloids at pH 7. This is attributed to a core-shell structure that includes the formation of a silicate-type of network, which is the only explanation for the strongly increased stability compared with the 'simple' surface modification. A structural model is shown in Fig. 9. As shown elsewhere,<sup>67</sup> these particles do not show any

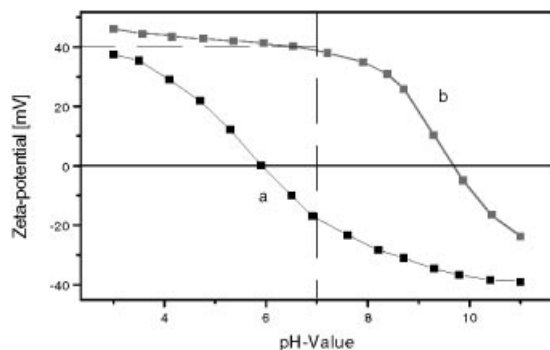


**Figure 8** Change of the zeta-potential by the amino coating; (a) untreated, after precipitation; (b) after modification and ultrasonic treatment.

hysteresis and are completely superparamagnetic. The positive zeta potential (+40 mV) of the particles is very important to obtain bonding to the surface of proteins and for a high stability under physiological conditions. These particles have been shown to be preferentially consumed by tumor cells very fast, and about 3 to 4 billion particles per cell are consumed but are not digested.<sup>118</sup> Even daughter cells produced by the tumor cells show the magnetic load. This means that the particles affect neither the cell division, nor the metabolism. By employing alternating magnetic fields, energy can be introduced into the cells and they can be destroyed by overheating (hyperthermal treatment). This opens up interesting perspectives for cancer treatment in the future.<sup>96,119</sup> In other investigations, iron oxide nanoparticles that have been surface-tailored for certain polymer matrices have been used for the fabrication of polymer matrix nanocomposites that are easily able to take up energy by heating, and those are presently being developed for many applications.<sup>120</sup> The use of sonochemistry seems to open up new preparation routes in multifunctional nanoparticle synthesis, and more investigations are necessary.

### 3.2 Nanocomposite hard coatings

The materials basis for nanocomposite hard coatings is broadly used for plastic surfaces. Inorganic-organic composites based on organoalkoxysilanes and other alkoxides have demonstrated their usefulness for hard coatings on eye-glass lenses.<sup>121</sup> It has been shown that the addition of nanoparticles, especially in combination with epoxy silanes, which act as an inorganic as well as an organic

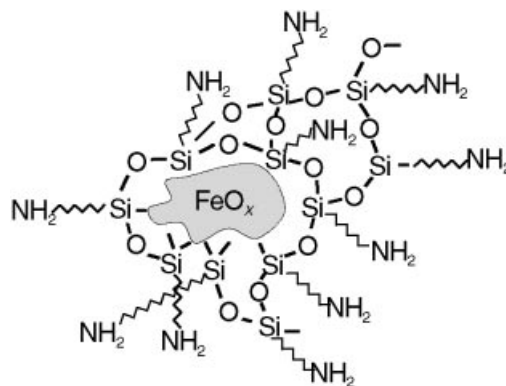


**Figure 9** Structural model of a core-shell  $\text{FeO}_x$  nanoparticle with silicate-type bonds between the surface modifier.

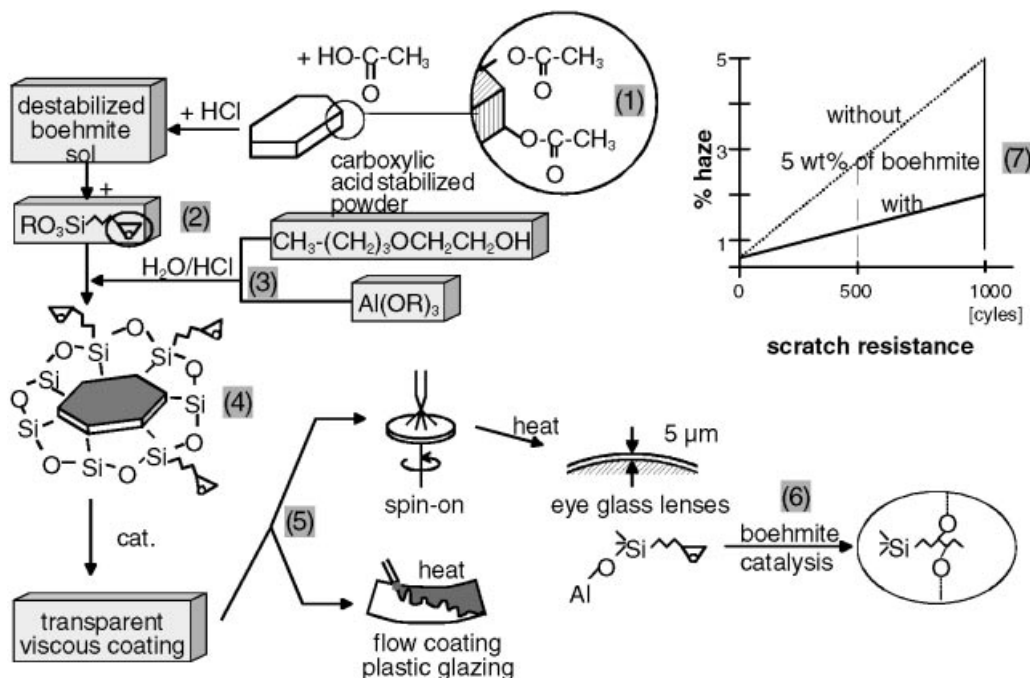


**Figure 10** Scheme of the preparation of a scratch-resistant boehmite nanocomposite coating and the effect of boehmite on the abrasion resistance.

crosslinking agent, leads to a substantial increase of the abrasion resistance of such systems without losing any transparency.<sup>122,123</sup>

For the application of these systems on polycarbonate as a transparent scratch-resistant coating, a very specific processing route has been developed. In general, the abrasion resistance of transparent coatings is measured by the decay of transmission by the scattered light after an abrasion treatment by the taber abrader test (two alumina-filled rubber wheels with 500 g load are abraded on a  $10 \times 10 \text{ cm}^2$  plate). The haze is determined after 500 or 1000 revolutions. For example, the haze value for float glass is about 1.5% after 1000 cycles, for UV-curable hard coatings for polycarbonate on automotive headlights it is about 15%, and for uncoated polycarbonate it is over 30% after 100 cycles. In order to obtain very high scratch-resistance values, a combination of several steps has been carried out, which is shown in Fig. 10 (after Refs 124 and 125). For the synthesis, a commercially available nanoparticulate boehmite surface modified with acetic acid (1) is dispersed in aqueous  $\text{HCl}$ . Here the 'boehmite acetate' is hydrolyzed to boehmite, which is followed by an increase of viscosity.<sup>126</sup> By addition of the

epoxysilane (2), a hydrolysis and condensation reaction on the boehmite surface takes place, leading to partially coated boehmite. The addition of  $\text{Al}(\text{OR})_3$  together with butoxyethanol leads to an  $\text{Al}(\text{OH})_2$ -butoxyethanolate, which is a stable intermediate and does not undergo further condensation without solvent removal and heat treatment. By addition of ethanol, the viscosity of the liquid is adjusted to 20–100 mPa s for carrying out dip and spin-on coating processes (5). At this point, as shown by NMR, the epoxy grouping is still unreacted. By heat treatment of these coatings above  $90^\circ\text{C}$ , the epoxy ring reacts to form a polymeric chain (6),<sup>126</sup> and by evaporation of butoxyethanol the additional formation of  $\text{AlOOH}$  from  $\text{Al}(\text{OH})_2$ -butoxyethanolate takes place. Comparing this process with the boehmite-free system, far higher abrasion-resistance values and almost no epoxy polymerization are observed. The difference in abrasion resistance is shown in (7) in Fig. 10. For the development of a practical product, several problems had to be solved: the optimization was carried out by statistical approaches. UV-protection has been obtained through addition of UV-absorbers (Tinuvin) and  $\text{CeO}_2$  nanoparticles. The process has been scaled up to batches of several hundred

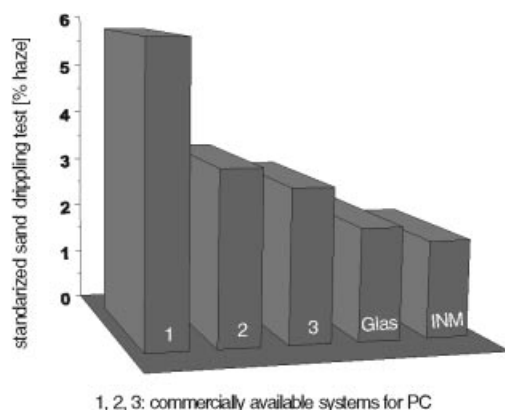


**Figure 11** Comparison of the nanocomposite coating on polycarbonate with glass and conventionally available coatings (data with permission of Bayer AG).

kilograms. The abrasion resistance of 2% haze meets specifications of automotive applications, and this system is being used as a basis for the development of plastic automotive glazing.

The sand-tripling shows lower haze numbers on these coatings, similar to those of float glass, and distinctively lower numbers than conventionally available polycarbonate coatings. This is shown in Fig. 11. This type of coating has been used as a basic layer for the development of interference layers by employing so-called polymerizable nanoparticles. The process is shown schematically in Fig. 12.<sup>127</sup> The coating materials are prepared through a sol-gel synthesis of  $\text{SiO}_2$  nanoparticles, which are reacted with methacryloxysilanes and by

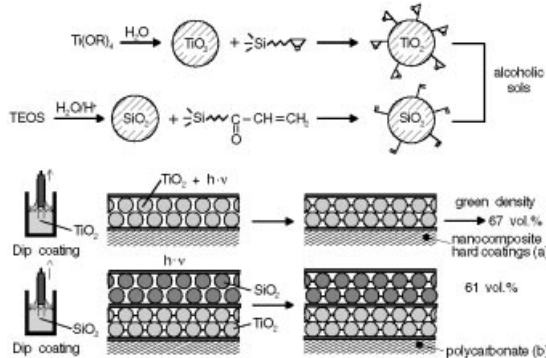


**Figure 12** Overview of the fabrication and application over the boehmite nanocomposite for the fabrication of abrasion-resistant overcoatings on hard coatings (a) or multilayer coatings for abrasion-resistant coatings on polycarbonate (b).

a sol-gel synthesis of  $\text{TiO}_2$  nanoparticles, which are coated with epoxy silanes, since with epoxy silanes colored complexes are formed. After the addition of a photoinitiator for the polymerization of the methacrylates and the polyaddition of the epoxides, a dip-coating process is carried out to form layer thicknesses in the range 150–300 nm. For optical purposes, interference layers according to the refractive index ( $\sim 1.90$  for  $\text{TiO}_2$  and 1.45 for  $\text{SiO}_2$ ) of the films have been developed. The refractive index of  $\text{TiO}_2$  is surprisingly high for only having undergone a photopolymerization process. This is due to the high green density of  $>90\%$ , completely unusual for ‘gels’. This, however, shows clearly the effect of the formation of the surface modification of nanoparticles, leading to rather dense Nanomer<sup>®</sup> structures; see Fig. 4. After photopolymerization, abrasion resistant surfaces with abrasion numbers down to about 1.5% haze at 120 or 130 °C curing temperature are obtained. This technique has been used for the fabrication of antireflective layers on plastic by dip- and spin-coating. For eye glass lenses, a so-called wet process antireflective coating has been developed that allows the fabrication of hard and antireflective coatings on plastic lenses with one and the same technique. Otherwise, hard coatings have to be employed by wet coatings and antireflection coatings by vacuum techniques.

### 3.3 Nanoparticles for hydrophobic-superhydrophobic surfaces

As shown in Refs 128 and 129, nanocomposites have been developed for the fabrication of low surface free energy coatings. In these investigations, it could be demonstrated that it is possible to obtain self-aligning coatings. With nanoparticles incorporated into the matrix, high abrasion resistance can be obtained. To promote good adhesion to different substrates, like metals, ceramics and plastics, adhesion promoters have been added. The self-aligning process up-concentrates the perfluorinated side chains of the silane at the surface, as proved by ESCA profiling and time-of-flight mass spectroscopy measurements. The results can be interpreted by a thermodynamically driven process of the system to minimize the interfacial or surface free energy. In the case of the fluorine-containing compounds, the free energy minimum of the fluorinated side chains can be achieved at the atmospheric side rather than at the polar interface to the substrate. This means that during the drying of



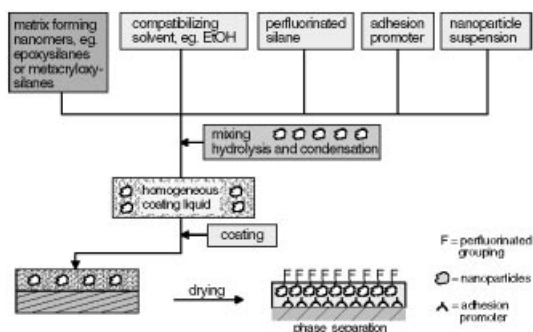


**Figure 13** Self-aligning process for the preparation of low surface free energy coatings.

mixtures, e.g. made from TEOS/MTOS epoxy or methacryloxy silanes optionally, perfluorinated silanes, e.g.  $(\text{RO})_3\text{Si}(\text{CH}_2)_2(\text{CF}_2)_8\text{CF}_3$  (FTS), and/or in combination with other alkoxides for the fabrication of inorganic networks, a diffusion process of the fluorinated silanes to the surface takes place. The scheme of the process is shown in Fig. 13.

Owing to the immiscibility of polar and fluorinated compounds, a maximum concentration of fluorinated silanes in the liquid mixture in the miscible regime exists. This can be determined by measuring the surface tension of the mixture as a function of the fluorine content. If the point of immiscibility is reached (critical micelle concentration, CMC), the surface tension reaches its minimum. The CMC of methacryloxy or epoxy silane based systems with TEOS, as a rule, ranges from 0.5 to 2 mol% of FTS.<sup>130</sup> For this reason, it was of interest to investigate how far the addition of nanoparticles influences the CMC. For this reason, an FTS-containing system was prepared by reacting

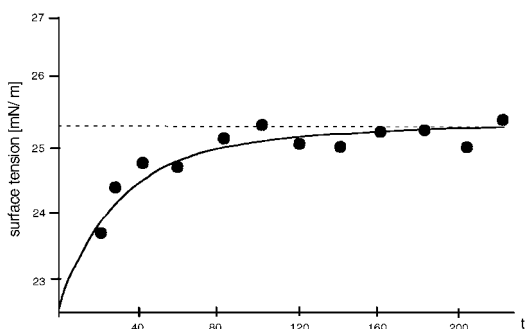


**Figure 14** Increase of the surface tension as a function of time in a system containing 10 wt% boehmite (~20 nm) and  $0.05 \text{ mol l}^{-1}$  of FTS.

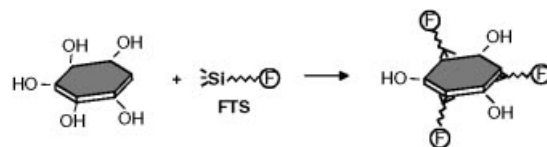


**Figure 15** Reaction of FTS for the formation of FTS-covered boehmite nanoparticles.

a nanoscale boehmite suspension in EtOH, with an FTS-containing alcoholic solution in 0.1 M HCl.<sup>131</sup> The total content of the boehmite was 10 wt% of the FTS  $0.05 \text{ mol l}^{-1}$ . It could be shown that the surface tension increases with time (Fig. 14). This can be explained by a bonding of the FTS to the  $\text{AlOOH}$  nanoparticles and a subsequent compatibilization of the FTS to the system, as shown in Fig. 15 in a structural model. If the surface tension is measured as a function of the FTS content of these systems with and without boehmite, the CMC is determined from the surface tension *versus* the FTS content plot by locating the intersection of the corresponding straight lines, as shown in Fig. 17<sup>132</sup> ( $\text{CMC} \equiv 2 \text{ mol l}^{-1}$  of FTS). However, it is very difficult to determine the variation of the CMC in the case of boehmite addition, because the curve cannot be divided into two clear sections. However, it clearly can be seen that it takes much higher concentrations of FTS to obtain surface tensions as low as without boehmite. This clearly points out that the CMC must be much higher in the case of boehmite-free systems, which again can be explained by the model depicted in Fig. 15.

These results have been used to develop gradient coatings for various applications. Owing to the

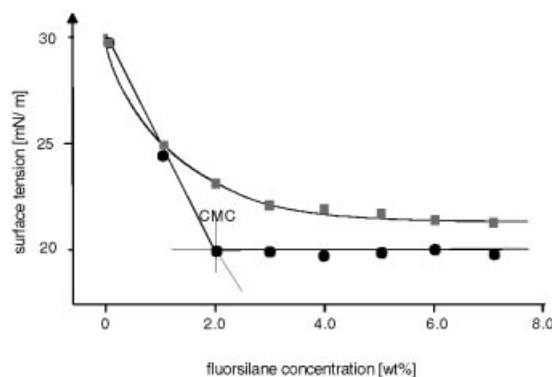


**Figure 16** Surface tension of a system containing 1.8 wt% of boehmite (20 nm) as a function of the FTS content (epoxy silane/TEOS/FTS composition according to Ref. 130).

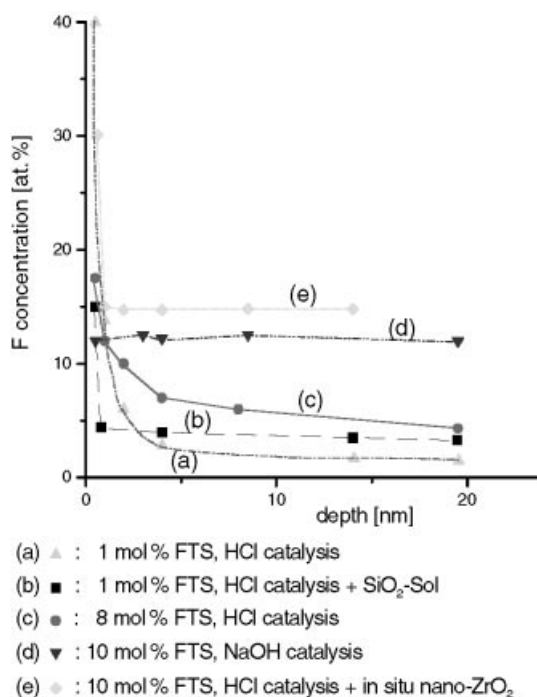


**Figure 17** ESCA profiles of various FTS-containing coatings.

thermodynamically driven gradient formation, the adhesion of films obtained by simple wet coating techniques could be solved for any type of substrate. Owing to the content of nanoparticles, the coatings are highly transparent. For applications, it is of importance to know about the fluorine concentration as a function of the distance to the surface. For these reasons, investigations<sup>133</sup> with different FTS concentrations under different reaction conditions have been carried out. The matrix system used for these experiments consists of methyl triethoxysilane (MTEOS), tetraethylorthosilicate (TEOS) and FTS. The FTS content was varied between 1 and 12 mol%. The fluorine profile was determined by ESCA analysis after repeated argon ion sputtering. Important results of the investigations are shown. Fig. 17 shows ESCA profiles of different systems. HCl-catalyzed systems with 1% FTS (a) without nanoparticles show high fluorine concentrations at the very top of the film of several nanometers only, and show a strong decay down to about 4% at 20 nm depth. The SiO<sub>2</sub> nanoparticle-containing system with 1 mol% FTS system with 28 mol% of SiO<sub>2</sub> (b) shows a distinctively lower surface concentration but a higher concentration at a depth of 20 nm. This indicates that the SiO<sub>2</sub> acts as a

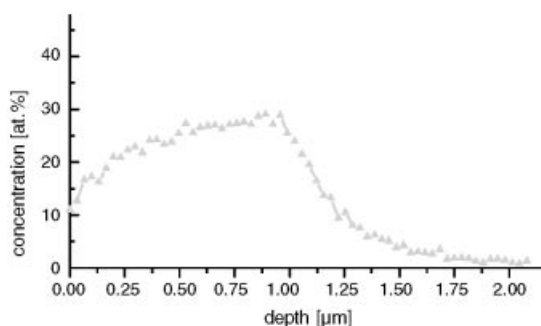


**Figure 18** SNMS profile of the NaOH-catalyzed MTEOS/TEOS/FTS system.

CMC-increasing agent in a similar way to boehmite. The NaOH-catalyzed system (d) shows a remarkably higher concentration at 20 nm, which is attributed to the fact that NaOH is superior to HCl as a condensation catalyst (c), immobilizing FTS by forming larger fluorine-containing entities and reducing their diffusion rate. The addition of Zr(OR)<sub>4</sub> alkoxides, which immediately forms n-ZrO<sub>2</sub>, leads to the highest average profiles. This can be explained by the ZrO<sub>2</sub> acting as a condensation catalyst<sup>123</sup> as well as an immobilizer for FTS at the same time. To find out how thick the fluorine-enriched layer is, an SNMS analysis of the NaOH system has been carried out. Fig. 18 shows the profile, which demonstrates the layer is about 1 μm thick. These investigations show that nanoparticles can be used for profile tailoring of gradient layers very advantageously. The contact angles of these layers with water vary between 90 and 110°. Owing to the low surface free energy, the adherence of dirt and soil is reduced drastically, and coatings with these properties can be considered as so-called easy-to-clean (ETC) coatings. Based on these results, many applications have been developed so far, e.g. on sanitary ware (Wondergliss®), for glass windows, for stainless steel surfaces or for mold release applications.

Meanwhile, a concept has been realized by additional incorporation of larger particles (80–100 nm). Coatings have been fabricated, and surface roughnesses of about 150–200 nm have been obtained. These (also self-aligning) systems show contact angles of about 140–160° with water and 100 to 110° with oil. The principle is shown in Fig. 19.<sup>134</sup> These rough surfaces lead to the so-called superhydrophobicity, a principle that is used by many plants, like plums, cabbage or the lotus plant, in order to get rid of moisture. This principle

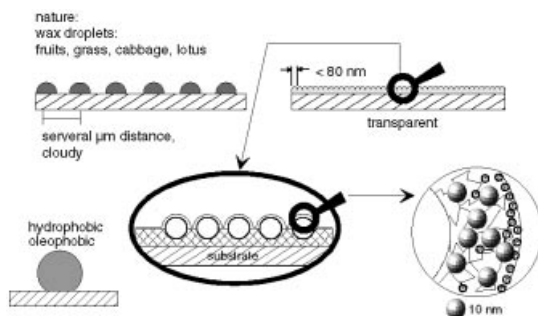


**Figure 19** Scheme of the principle fluorine-containing superhydrophobic systems by a self-micropatterning process using nanoparticles as a patterning tool.

at present is being developed further for specific application.

#### 4. DISCUSSION

For the transfer of basic results into industrial applications, a specific approach has to be realized. Besides the fulfilling of all specific requirements defined by the customer, which, in general, can be carried out under laboratory conditions, in most cases a technology development has to be carried out, since the majority of the industrial appliers of materials are neither familiar with chemical processing and synthesis of materials nor able to develop the appropriate application technologies; but of course, they are highly interested in novel products. For this reason, a well-organized 'vertical interdisciplinarity' is linking together chemists, physicists, engineers and production technologists to develop customer-oriented new technologies beginning at the materials basis. Using this approach, in combination with the appropriate technological equipment, is an indispensable pre-requirement to process nanomaterials to products close to the market as described above.

#### 5. OUTLOOK

There is a huge potential for nanostructured materials produced through chemistry in the future. The large potential is mainly based on the needs of the end users. In order to exploit these potentials, developments close to the markets starting from basic research are necessary. If this becomes more

common, nanostructured materials will obtain a large and widespread significance in industry.

#### REFERENCES

- Gleiter H. *Nanocrystalline Materials*, *Prog. Mater. Sci.* 1989; **33**: 223–315.
- Gleiter H. *Mater. Sci. Forum* 1995; **189–190**: 67–80.
- Gleiter H. *Nanostruct. Mater.* 1995; **6**(1–4): 3–14.
- Siegel RW. *Nanomater.: Synth. Prop. Appl.* 1996; 201–218.
- Siegel RW. *Adv. Top. Mater. Sci. Eng.* 1991; 273–288.
- Niihara K. *Seramikkusu* 1992; **27**(4): 293–299.
- Stöber W, Fink A, Bohn E. *Colloid Interface Sci.* 1968; **26**: 62–69.
- Stern O. *Z. Elektrochem.* 1924; **30**: 508.
- Oguir Y, Riman RE, Bowen HK. *J. Mater. Sci.* 1988; **23**(8): 2897–2904.
- Hausner H, Roosen A. *Adv. Ceram. Mater.* 1988; **3**(2): 131–137.
- Sanchez C, Lebeau BP. *Appl. Opt.* 1996; **5**(5): 689–699.
- Koch T, Mennig M, Schmidt H. *CIMTEC* 1998.
- Mark JE, Jiang CY. *Macromolecules* 1984; **17**(12): 2613–2616.
- Wen J, Mark JE. *Rubber Chem. Technol.* 1994; **67**(5): 806–819.
- Garrido L, Mark JE, Sun CC, Ackerman JL, Chang C. *Macromolecules* 1991; **24**(14): 4067–4072.
- Krug H, Müller P, Oliveira PW, Schmidt H. *DE* 19719948, 1998.
- Lange F. *International Symposium on Molecular Level Designing of Ceramics*. Team of the NEDO International Joint Research Program: Nagoya (eds), 1991; 14.
- Gan F. *J. Sol–Gel Sci. Technol.* 1998; **13**(1–3): 559–563.
- Sanchez C, Ribot F, Lebeau B. *J. Mater. Chem.* 1999; **9**(1): 35–44.
- Saravanamuttu K, Andrews MP, Najafi SI. *SPIE* 1998; **3417**: 19–24.
- Andrews MP, Saravanamuttu K, Touam T, Sara R, Du XM, Najafi SI. *SPIE* 1998; **3282**: 50–58.
- Lal M, Joshi M, Kumar DN, Friend CS, Winiarz J, Asefa T, Kim K, Prasad PN. *Mater. Res. Soc. Symp. Proc.* 1998; **519**: 217–225.
- Wong HP, Dave BC, Leroux F, Harreld J, Dunn B, Nazar LF. *J. Mater. Chem.* 1998; **8**(4): 1019–1027.
- Cordoncillo E, Viana B, Escribano P, Sanchez C. *J. Mater. Chem.* 1998; **8**(3): 507–509.
- Blanc D, Peyrot P, Sanchez C, Gonnet C. *Opt. Eng. (Bellingham, Wash.)* 1998; **37**(4): 1203–1207.
- Friend CS, Lal M, Biswas A, Winiarz J, Zhang L, Prasad PN. *SPIE* 1998; **3469**: 100–107.
- Etienne P, Coudray P, Moreau Y, Porque J. *J. Sol–Gel Sci. Technol.* 1998; **13**(1–3): 523–527.
- Chen Y, Chan HLW, Choy CL. *ISAF '96, Proceedings of the IEEE International Symposium on Applied Ferroelectrics, 10th Annual Meeting, Hong Kong, 1996*; 619–622.

29. Hirano S, Yogo T, Kikuta K, Yamada S. *Ceram. Trans.* 1996; **68**: 131–140.
30. Zhang Q, Chan HLW, Zhou Q, Choy CL. *Chin. Sci. Bull.* 1998; **43**(2): 111–114.
31. Chen Y, Chan HLW, Choy CL. *Thin Solid Films* 1998; **323**(1–2): 270–274.
32. Chen Y, Chan HLW, Choy CL. *J. Korean Phys. Soc.* 1998; **32** (Suppl.): 1072–1075.
33. Chen Y, Chan HLW, Choy CL. *J. Am. Ceram. Soc.* 1998; **81**(5): 1231–1236.
34. Zhang Q, Chan HLW, Choy CL. *Composites, Part A* 1998; **30**(2): 163–167.
35. Zhang Q, Chan LW, Zhou Q, Choy CL. *Mater. Res. Innovations* 1999; **2**(5): 283–288.
36. Chan HLW, Lau ST, Kwok KW, Zhang Q, Zhou QF, Choy CL. *Sens. Actuators A* 1999; **75**(3): 252–256.
37. Mark JE. *International SAMPE Technical Conference (Diversity into the Next Century)*. 1995; **27**: 539–548.
38. Sarwar MI, Ahmad Z. Advanced Materials—97, [Proceedings International Symposium], 5th, Khan MA (ed.). Dr A. Q. Khan Research Laboratories Kahuta: Rawalpindi, Pak, Islamabad, 1997; 73–77.
39. Motomatsu M, Takahashi T, Nie H-Y, Mizutani W, Tokumoto H. *Polymer* 1997; **38**(1): 177–182.
40. Gerard JF, Kaddami H, Pascault JP. Extended Abstracts—EUROFILLERS 97, *International Conference Filled Polym. Fillers*, 2nd Lyon, 1997; 407–410.
41. Reynaud E, Gauthier C, Perez J. *Rev. Metall./Cah. Inf. Tech.* 1999; **96**(2): 169–176.
42. Mauritz KA, Stefanithis ID, Davis SV, Scheetz RW, Pope RK, Wilkes GL, Huang H-H. *J. Appl. Polym. Sci.* 1995; **55**(1): 181–190.
43. Shao PL, Mauritz KA, Moore RB. *Polym. Mater. Sci. Eng.* 1995; **73**: 427–428.
44. Shao PL, Mauritz KA, Moore RB. *Chem. Mater.* 1995; **7**(1): 192–200.
45. Deng Q, Cable KM, Moore RB, Mauritz KA. *J. Polym. Sci. Part B: Polym. Phys.* 1996; **34**(11): 1917–1923.
46. Young SK, Deng Q, Mauritz KA. *Polym. Mater. Sci. Eng.* 1996; **74**: 309–310.
47. Harmer MA, Farneth WE, Sun Q. *J. Am. Chem. Soc.* 1996; **118**(33): 7708–7715.
48. Robertson MAF, Mauritz KA. *J. Polym. Sci. Part B: Polym. Phys.* 1998; **36**(4): 595–606.
49. Honma I, Hirakawa S, Yamada K, Bae JM. *Solid State Ionics* 1999; **118**(1–2): 29–36.
50. Dahmouche K, Santilli CV, Pulcinelli SH, Craievich AF. *J. Phys. Chem. B* 1999; **103**(24): 4937–4942.
51. Hu Z, Slaterbeck AF, Seliskar CJ, Ridgway TH, Heinemann WR. *Langmuir* 1999; **15**(3): 767–773.
52. Nunes SP, Schultz J, Peinemann K-V. *J. Mater. Sci. Lett.* 1996; **15**(13): 1139–1141.
53. Hu Q, Marand E, Dhingra S, Fritsch D, Wen J, Wilkes G. *J. Membr. Sci.* 1997; **135**(1): 65–79.
54. Malla PB, Komarneni S. *Mater. Res. Soc. Symp. Proc.* 1993; **286**: 323–334.
55. Okada A, Usuki. *Mater. Sci. Eng. C* 1995; **3**(2): 109–115.
56. Gray DH, Hu S, Juang E, Gin DL. *Adv. Mater.* 1997; **9**(9): 731–736.
57. Olivera-Pastor, Maireles-Torres P, Rodriguez-Castellon E, Jimenez-Lopez A, Cassagneau T, Jones DJ, Roziere J. *Chem. Mater.* 1996; **8**(8): 1758–1769.
58. Ukrainczyk L, Bellman RA, Smith KA, Boyd JE. *Mater. Res. Soc. Symp. Proc.* 1997; **457**: 519–524.
59. Ukrainczyk L, Bellman RA, Anderson AB. *J. Phys. Chem. B* 1997; **101**(4): 531–539.
60. Chakravorty D. In *New Materials*, Joshi SK (ed.). Narosa: New Delhi, India, 1992; 170–194.
61. Nakamura O, Saito Y, Nakamura H, Asai T, Ado K, Haruta M, Kobayashi T, Tsubota S, Sakurai H et al. *Osaka Kogyo Gijutsu Shikensho Hokoku* 1992; **386**: 1–180.
62. Roy R. *Mater. Res. Soc. Symp. Proc.* 1993; **286**: 241–250.
63. Roy R. *Trans. Mater. Res. Soc. Jpn. B* 1994; **19**: 719–728.
64. Lantelme B, Dumon M, Mai C, Pascault JP. *J. Non-Cryst. Solids* 1996; **194**(1–2): 63–71.
65. Robertson MAF, Mauritz KA. *Polym. Prepr. (Am. Chem. Soc. Div. Polym. Chem.)* 1996; **37**(2): 248–249.
66. Courtois C, Rabih A, O'Sullivan D, Leriche A, Thierry B. *Key Eng. Mater.* 1997; **132–136**: 1010–1013.
67. Matejka L, Plestil J. Macromolecules Symposium, International Symposium on Polycondensation, Related Processes and Materials, 1996, Prague, Czech Republic, 1997; 191–196.
68. Tutorskii IA, Tkachenko TE, Malyavskii NI. *Proizvod. Ispol'z. Elastomerov* 1997; **8**: 6–10.
69. Ulibarri TA, Derzon DK, Wang LC. Annual Technical Conference—Society of Plastics Engineers, 55th, 1997; **2**: 1925–1930.
70. Mohseni M, James PF, Wright PV. *J. Sol–Gel Sci. Technol.* 1998; **13**(1–3): 495–497.
71. Hay J, Raval H, Porter D. *Chem. Commun. (Cambridge)* 1999; (1): 81–82.
72. Yano S, Iwata K, Kurita K. *Mater. Sci. Eng. C* 1998; **6**(2–3): 75–90.
73. Senna M. *Electrical Phenomena at Interfaces, Surfactant Science Series*, 76. Yokohama, Japan, 1998; 503–517.
74. Kang J, Park SH, Kwon HY, Park DG, Kim SS, Kweon H-J, Nam SS. *Bull. Korean Chem. Soc.* 1998; **19**(5): 503–506.
75. Ahmad Z, Sarwar MI, Krug H, Schmidt H. *Int. J. Polym. Mater.* 1998; **39**(1–2): 127–140.
76. Asif KM, Sarwar MI, Rafiq S, Ahmad Z. *Polym. Bull. (Berlin)* 1998; **40**(4–5): 583–590.
77. Sharp KG. *Mater. Res. Soc. Symp. Proc.* 1998; 123–135.
78. Lebeau B, Sanchez C. *Curr. Opin. Solid State Mater. Sci.* 1999; **4**(1): 11–23.
79. Saravanamuttu K, Du XM, Najafi SI, Andrews MP. *Can. J. Chem.* 1998; **76**(11): 1717–1729.
80. Sanchez C, Lafuma A, Rozes L, Nakatani K, Delaire JA, Cordoncillo E, Viana B, Escribano P. *Organic–Inorganic Hybrid Materials for Photonics, SPIE* 1998; **3469**: 192–200.
81. Tagaya H, Nagaoka T, Kuwahara T, Karasu M, Kadokawa J-I, Chiba K. *Micropor. Mesopor. Mater.* 1998; **21**(4–6): 395–402.
82. Messersmith PB, Giannelis EP. *Chem. Mater.* 1994; **6**(10): 1719–1725.

83. Reichert P, Kressler J, Thomann R, Muehlhaupt R, Steppelmann G. *Acta Polym.* 1998; **49**(2–3): 116–123.
84. Heckmann W, Ramsteiner F, Mehler C. Morphology of polyamide nanocomposites by transmission electron microscopy (TEM) and electron spectroscopic imaging (ESI), oral presentation at Fall 2000 ACS National Meeting, Washington, DC, 20–24/08/2000.
85. Sakka Y, Sodeyama K. *American Ceramic Society* 1998; 83.
86. Matijevic E. *Langmuir* 1994; **10**(1): 8–16.
87. Matijevic E. *NATO ASI Ser.*, 1996; **12**: 1–2.
88. Matijevic E, Her YS. *NATO ASI Ser.*, 1996; **18**: 189–202.
89. Scherer GW, Brinker C. *Sol–Gel Science: the Physics and Chemistry of Sol–Gel Processing*, Jeffrey (ed.). Academic Press: San Diego, 1990.
90. Henglein A. *Chem. Rev.* 1989; 1861–1873.
91. Henglein A, Fojtik A. *Ber. Bunsenges. Phys. Chem.* 1987; **91**(4): 441–446.
92. Henglein A, Gutierrez M. *Ber. Bunsenges. Phys. Chem.* 1983; **87**: 852–885.
93. Schmid G. *Bull. Pol. Acad. Sci. Chem.* 1998; **46**(3): 229–235.
94. Schmid G, Peschel S. *New J. Chem.* 1998; **22**(7): 669–675.
95. Schmid G, Klein N, Morun B, Lehnert A, Malm S, Olle J. *Pure Appl. Chem.* 1990; **62**(6): 1175–1177.
96. Schmidt H, Nonninger R. *Proceedings of Fine, Ultrafine and Nano Powders '98*, New York, 1998.
97. Schmidt HK. *Kona Powder and Particle* 1996; **14**: 92–103.
98. Schmidt HK, Nass R, Burgard D, Nonninger R. *Mater. Res. Soc. Symp. Proc.* 1998; **520**: 21–31.
99. Schmidt H. *Mater. Funct. Des. Proc. Eur. Conf. Adv. Mater. Proce. Appl.*, 5th, 1997.
100. Mennig M, Schmitt M, Becker U, Jung G, Schmidt H. *SPIE* 1994; **2288**: 120–129.
101. Spanhel L, Arpac E, Schmidt H. *J. Non-Cryst. Solids* 1992; **147**: 657–662.
102. Henglein A, Fojtik A, Weller H. *Ber. Bunsenges. Phys. Chem.* 1987; **91**(4): 441–446.
103. Burgard D, Naß R, Schmidt H. DE 19515820 A1, 1996.
104. Roy R, Komarneni S. Report (AD), 1993; 121.
105. Komarneni S, Menon VC *et al. Ceram. Trans.* 1996; **62**: 37–46.
106. Sanchez C, Livage J, Henry M, Babonneau F. *J. Non-Cryst. Solids* 1998; **100**: 65.
107. Naß R, Schmidt H. *Powder Processing Science*. Deutsche Keramische Gesellschaft: Köln, 1989; 69.
108. Schiestel T, Schirra H, Gerwahn J, Lesniak C, Kalaghi-Nafchi A, Sameti M, Borchard G, Haltner E, Lehr CM, Schmidt H. *Mater. Res. Soc. Proc.* 1998; 65–71.
109. Kneuer C, Sameti M, Haltner EG, Schiestel T, Schirra H, Schmidt H, Lehr CM. *Int. J. Pharm.* in press.
110. Mennig M. Personal communication, to be published later.
111. Pileni MP, Feltin N, Moumen N. *Sci. Clin. Appl. Magn. Carriers. Proceedings of International Conference 1st* 1997; 117–133.
112. Feltin N, Pileni MP. *Langmuir* 1997; **13**(15): 3927–3933.
113. Monroe LD, Erickson DD, Wilson DM, Wood TE. US 5611829, 1995.
114. Erickson DD, Monroe LD, Wood TE, Wilson DM. US 5645619, 1996.
115. Sieber W. WO 96/02060, 1996.
116. Schmidt H, Lesniak Chr, Schiestel T. *F. Part. Sci. Tech.* 1996; 23–642.
117. Lesniak Chr, Schiestel T, Naß R, Schmidt H. *Mater. Res. Soc. Proc.* 1997; 122–134.
118. Jordan A, Scholz R, Wust P, Schirra H, Schiestel T, Schmidt H, Felix R. *J. Magn. Magn. Mater.* 1999; **194**(1–3): 185–189.
119. Lesniak C, Schiestel T, Schmidt H, Jordan A. E 19726282 A1, 1997.
120. Nonninger R. In preparation.
121. Schmidt H, Seiferling B, Philipp G, Deichmann K. *Proc. Ultrastruc. Proc. Ceram. Glas. Comp.* John Wiley & Sons: San Diego, 1988; 651–660.
122. Kasemann R, Geiter E, Schmidt H, Arpac E, Wagner G, Gerhard V. DE 4338361 A1, 1995.
123. Schmidt H, Kasemann R, Burkhart T, Wagner G, Arpac E, Geiter E. *ACS Symp. Proc. Ser.* 585; 331–347.
124. Kasemann R, Schmidt H, Wintrich E. *Mater. Res. Soc. Proc.* 1994; **346**: 915–921.
125. Braune B, Geiter E, Krug H, Müller P, Schmidt H. DE 19630100 A1, 1996.
126. Geiter E. Dissertation.
127. Mennig M, Oliveira PW, Frantzen A, Schmidt H. *Proceedings of 2nd ICCG*, 1998.
128. Schmidt H, Kasemann R. DE 4118184, 1991.
129. Schmidt H, Brück S, Kasemann R. *Bol. Soc. Esp. Cer. C* 1992; **31**: 75–80.
130. Sepeur S. *Masters Thesis*, University of the Saarland, 1994.
131. Krämer P. *Master Thesis*, University of the Saarland, 1997.
132. Sepeur S. Personal communication, to be published.
133. Schmidt H, Schmitjes O. Personal communication, to be published.
134. Schmidt H *et al.* Personal communication, patent pending, to be published later.